



Limitations of estimating branch volume from terrestrial laser scanning

Christopher Morhart¹ · Zoe Schindler¹ · Julian Frey¹ · Jonathan P. Sheppard¹ · Kim Calders² · Mathias Disney^{3,4} · Felix Morsdorf⁵ · Pasi Raunonen⁶ · Thomas Seifert^{1,7}

Received: 26 May 2023 / Revised: 9 November 2023 / Accepted: 12 December 2023 / Published online: 14 January 2024
© The Author(s) 2024

Abstract

Quantitative structural models (QSMs) are frequently used to simplify single tree point clouds obtained by terrestrial laser scanning (TLS). QSMs use geometric primitives to derive topological and volumetric information about trees. Previous studies have shown a high agreement between TLS and QSM total volume estimates alongside field measured data for whole trees. Although already broadly applied, the uncertainties of the combination of TLS and QSM modelling are still largely unexplored. In our study, we investigated the effect of scanning distance on length and volume estimates of branches when deriving QSMs from TLS data. We scanned ten European beech (*Fagus sylvatica* L.) branches with an average length of 2.6 m. The branches were scanned from distances ranging from 5 to 45 m at step intervals of 5 m from three scan positions each. Twelve close-range scans were performed as a benchmark. For each distance and branch, QSMs were derived. We found that with increasing distance, the point cloud density and the cumulative length of the reconstructed branches decreased, whereas individual volumes increased. Dependent on the QSM hyperparameters, at a scanning distance of 45 m, cumulative branch length was on average underestimated by –75%, while branch volume was overestimated by up to +539%. We assume that the high deviations are related to point cloud quality. As the scanning distance increases, the size of the individual laser footprints and the distances between them increase, making it more difficult to fully capture small branches and to adjust suitable QSMs.

Keywords Remote sensing · LiDAR · TLS · QSM · Above-ground volume · European beech

Communicated by Tianjian Cao.

Christopher Morhart and Zoe Schindler have contributed equally to the work.

✉ Christopher Morhart
christopher.morhart@wwd.uni-freiburg.de

Zoe Schindler
zoe.schindler@wwd.uni-freiburg.de

Julian Frey
julian.frey@wwd.uni-freiburg.de

Jonathan P. Sheppard
jonathan.sheppard@wwd.uni-freiburg.de

Kim Calders
kim.calders@ugent.be

Mathias Disney
mathias.disney@ucl.ac.uk

Felix Morsdorf
felix.morsdorf@geo.uzh.ch

Pasi Raunonen
pasi.raunonen@tuni.fi

Thomas Seifert
thomas.seifert@wwd.uni-freiburg.de

¹ Chair of Forest Growth and Dendroecology, University of Freiburg, Freiburg, Germany

² CAVELab - Computational and Applied Vegetation Ecology, Department of Environment, Ghent University, Ghent, Belgium

³ UCL Department of Geography, London, UK

⁴ NERC National Centre for Earth Observation (NCEO-UCL), Leicester, UK

⁵ Spatial Genetics, Remote Sensing Laboratories, Department of Geography, University of Zurich, Zurich, Switzerland

⁶ Computing Sciences, Tampere University, Tampere, Finland

⁷ Department of Forest and Wood Science, Stellenbosch University, Stellenbosch, South Africa

Introduction

Knowledge about the above-ground volume of single trees and complete forest stands is of high importance as basis for multiple decisions for management as well as for varied scientific questions. For example, volume estimates of stands can be used to calculate thinning intensities and sustainable harvesting approaches. In recent years, especially in the context of climate change mitigation, information about biomass-derived sequestered carbon has gained more and more attention. Both volume and biomass are traditionally determined by destructive sampling of whole trees or parts of trees (Seifert and Seifert 2014). These methods, however, are very laborious, time-consuming, costly and inherent of their destructive nature, render repeated measurements over time impossible. A non-destructive method for estimating tree biomass is the use of species-specific allometric functions that are based on simple geometric measurements such as tree diameter at breast height (DBH) and tree height (Picard et al. 2012; Roxburgh et al. 2015; Paul et al. 2016). These functions, however, are still usually parameterised based on measurements of destructively harvested trees. As such, they are only able to provide reliable estimates within clear boundaries: (1) comparability of site and stand conditions (such as climate, soil, stand density, and species composition) between the sample and the subject trees, (2) the estimated trees need to be within the calibration range according to the dimensions of the predictor variable and must be of the same species and (3) the estimated trees shall not be of an atypical growth form or with defects such as with a low fork or with a hollow trunk. A recent study by Calders et al. (2022) has shown how neglecting the underlying assumptions of allometric functions can lead to substantial bias in the estimation of above-ground biomass in forests. Furthermore, the choice of analysis methods, model selection and ignoring model assumptions can lead to inaccurate and biologically implausible allometric functions (Sileshi 2014; Picard et al. 2015). For this reason, allometric functions cannot be considered a universal tool for estimating tree volume or biomass for any tree or stand alone.

An alternative to destructive sampling and allometric modelling are the estimation of volume or biomass utilising remote sensing. Satellite data or laser scans from aerial platforms or unmanned aerial vehicles (UAVs) can be used to estimate stand volume (e.g. Maack et al. 2016; Puliti et al. 2020). However, corresponding individual tree estimates are subject to high uncertainty. One of the most promising methods for assessing the above-ground volume and several more single tree parameters is terrestrial laser scanning (TLS) (Vonderach et al. 2012; Astrup et al. 2014;

Calders et al. 2015; Hackenberg et al. 2015; Raunonen et al. 2015; Sheppard et al. 2017; Disney et al. 2018; Bohn Reckziegel et al. 2022; Schindler et al. 2023a, 2023b). TLS is a LiDAR (*Light Detection And Ranging*) based technique that produces high-resolution 3D point clouds of trees with up to several million points per tree. Since the early 2000s, this technology has been used within forestry applications for various purposes, such as extracting forest inventory parameters (Liang et al. 2016), assessing carbon stocks (Schindler et al. 2023b), quantifying forest structure (Ehbrecht et al. 2016), estimating leaf area index and light variability (Antonarakis et al. 2010; van der Zande et al. 2010; Roskopf et al. 2017; Bohn Reckziegel et al. 2021), measuring crown structure (Pretzsch et al. 2011), quantifying tree growth (Sheppard et al. 2017; Yrttimaa et al. 2023), classifying tree species (Haala et al. 2004; Othmani et al. 2013), assessing wood quality (Pyörälä et al. 2019), estimating leaf angles (Stovall et al. 2021) and mapping microhabitats (Frey et al. 2020) and bark surface structure (Kretschmer et al. 2013). Additionally, TLS has been utilised for ecological applications such as assessments of biodiversity (Knuff et al. 2020; Helbach et al. 2022; Rappa et al. 2022) and microclimate (Ehbrecht et al. 2019; Kolbe et al. 2022). Often, the collected 3D data are used as basis for the calculation of geometric primitives such as spheres, cones or cylinders for better handling and eased calculation. From these quantitative structural models (QSMs), geometric and volumetric information, as well as topological properties, can be derived (Raunonen et al. 2013; Hackenberg et al. 2014; Åkerblom et al. 2015). Combining the volumetric data with density and carbon content information enables the estimation of above-ground biomass and carbon stocks (Calders et al. 2015; Disney et al. 2018).

Many previous studies show the good agreement of QSM-derived volume or biomass estimates with manual measurements of stem diameters and tree height (Liang et al. 2016; Pyörälä et al. 2019), dependent on scanning technology, number of scans, species and stand structure (Brede et al. 2017). While some studies indicated an underestimation of volume or biomass (Gonzalez de Tanago et al. 2018), other studies found QSMs to overestimate these (Calders et al. 2015; Raunonen et al. 2015). Previous studies often evaluated the accuracy of their TLS derived volume or biomass estimates based on single tree or even stand level without regarding different branches and stem diameter classes separately. Recently, Demol et al. (2022) investigated the accuracy of QSM volume estimates on two trees at the level of branch detail. They found the QSMs to provide a total volume overestimation of 38% up to 52%. Branches with less than 5 cm in diameter contributed to about 80% of the respective overestimation in the study. They argue the overestimation to be mainly caused by misaligned point clouds and scattering

errors due to partial returns. Nevertheless, they emphasise the need for further research to uncover the mechanisms leading to inaccuracies. In a study by Abegg et al. (2023), the effect of object diameters on tree volume estimates was investigated using simulated point clouds. They found the volume of small branches with a diameter below 7 cm to be severely overestimated and suggest that this effect might be caused by noise resulting from the scanning distance. While these small tree parts were overestimated by 110% for small trees, their volume was underestimated by 50% for larger trees, probably due to occlusion effects. Such a compensation of volume overestimation by occlusion was as well observed by Kükenbrink et al. (2021) in a TLS dataset of 55 destructively sampled urban trees. It is very likely, though, that this effect does not generalise well across different tree species and growing conditions.

Since the fitting process of QSMs is mostly data-driven and currently depends on 3D point coordinates only, the geometric primitives are fitted to all points, regardless of their plausibility (Raumonen et al. 2013; Wilkes et al. 2021; Raumonen and Åkerblom 2022). Consequently, that means that the QSMs are only as good as the point clouds they are derived from. To obtain perfect QSMs, perfect point clouds without erroneous points are a prerequisite. The quality of point clouds obtained using LiDAR devices is influenced by many factors, e.g. laser scanning technique and features of the scanned object (Boehler et al. 2003). In addition to these factors, other sources of error can occur when scanning in forest conditions, such as unfavourable weather (wind and precipitation), occlusion by plants and large scanning distances due to the size of the objects. For most of these factors, there is currently only insufficient knowledge about their impact on volume estimates and the underlying mechanisms. Most previous studies have been conducted on whole trees and under uncontrolled conditions, making it difficult to isolate the effects of the individual factors.

In conclusion, despite frequent application in various research fields and despite technological progress, there are still unexplored uncertainties and unresolved inaccuracies when using TLS and QSMs. For example, when laser beams only partially hit objects, recorded points may be shifted away from the object towards the centre of the emitted light pulse and not adequately represent the object surface (Wilkes et al. 2021). As the distance between the scanner and the object increases, the size of the laser footprint and thus the proportion of partial hits increase, while the total number of laser pulses per area decreases at the same time (Abegg et al. 2021). Partial hits and large footprints are known to affect point cloud quality, but the impact of scanning distance on volume estimates derived from TLS and QSMs is yet to be quantified in real data. In a previous study by Abegg et al. (2023), the effect of distance noise on volume estimates was quantified. However, they did not

evaluate the effects as a function of scanning distance and used simulated point clouds only.

With increasing tree height, branch diameter generally decreases along the vertical axis. Branches are positioned progressively higher in the crown and more distant to the ground, and thus also from the TLS device. This leads not only to more self-occlusion by the trees themselves (Abegg et al. 2017), but also to increasing distance-dependent errors, especially for small-diameter branches (Abegg et al. 2021).

In this paper, we aim to investigate the effect of the distance between TLS scan positions and scanned branches on the QSM-based estimates of branch volume and length. We chose to use European beech (*Fagus sylvatica* L.) branches for our study, as it is not only one of the most important European tree species, but also has exceptionally thin branches with minimum diameters of only a few millimetres. Moreover, since European beech can grow up to around 40 m in height (Packham et al. 2012), this, in combination with the fine branching structure, is especially challenging for the TLS technique. For our experiment, ten beech branches without leaves were scanned from different distances simulating vertical height differences between scanner and branches as part of the canopy. We used leafless branches, as deciduous trees are usually scanned in winter to reduce occlusion effects arising from leaves. To exclude any disturbing weather conditions such as wind or rain, which can lead to measurement errors (Krok et al. 2020), the branches were scanned under controlled, near-optimal conditions within a sports hall. Using different sampling distances, a comparison of QSM estimates with the estimates of the best possible point clouds obtained by multiple close-range scans is given to make a solid assessment of possible errors. To exclude influencing factors such as wind and precipitation, we scanned indoors.

Our research hypotheses, formulated as alternative hypotheses, are:

- (1) With increasing distance between TLS scan position and scanned branches, cumulative branch length estimates decrease due to a lower point cloud density.
- (2) With increasing distance between TLS scan position and scanned branches, branch volume estimates increase.

Methods

TLS data collection

The ten sample branches were collected in a nearby beech-dominated forest under leafless conditions. We concentrated on the last metres of branches containing the smallest twigs. On average, the sample branches had a width of 2.1 m, a



Fig. 2 **a** Laser beam radius and diameter (mm) of the RIEGL VZ-400i depending on the distance to the scanner. **b** Laser beam diameter (mm) and distance between the centres of the laser beams (mm) and number of full hits on a target area of 9 cm × 9 cm with increasing

scanning distance (left: 5 m, centre: 20 m, and right: 45 m), assuming a horizontal and vertical resolution of 0.04°. The red circles show the size of single laser footprints at the respective scanning distance on a 9 cm × 9 cm flat surface

of hyperparameters prior to computation. Here, the hyperparameters were optimised for each branch scanned from each distance by computing five QSMs each for 24 different hyperparameter combinations (2, 4 and 3 values for *PatchDiam1*, *PatchDiam2Min*, and *PatchDiam2Max*, respectively; Appendix, Table 3) defined by an in-built function recommended in the software's manual (Raumonen and Åkerblom 2022). The function selects parameter ranges based on the stem base radius and point cloud density. Since some of the point clouds did not converge, a minimum stem diameter of 1 cm was implemented in that function to prevent the selection of unrealistic hyperparameters. TreeQSM does not produce deterministic results; therefore, multiple models per point cloud must be computed to obtain robust estimates (Raumonen and Åkerblom 2022). For each branch and experimental scanning distance, 50 QSMs were computed using the respective optimised hyperparameter set that previously yielded the smallest average distance between points and cylinders (in the following “optimised”). The same procedure was conducted on the data from the

close-range scans to produce the benchmarking dataset (in the following “benchmark”). A further 50 QSMs were computed for each branch and experimental scanning distance, using a set of pre-defined parameters selected based on prior experiences with TreeQSM (in the following “fixed”, *PatchDiam1* = 0.05, *PatchDiam2Min* = 0.005, *PatchDiam2Max* = 0.02, *BallRad1* = 0.07, *BallRad2* = 0.03). For all QSMs, the minimum cylinder radius was manually set to 1 mm to account for the small minimum diameters of the sampled branches (*MinCylRad* = 0.001).

Statistical analysis

All statistical analyses were conducted in R v4.2.1 (R Core Team 2022). For each branch, scanning distance and hyperparameter set, the variables derived from the QSMs were averaged using the arithmetic mean. In the following, we refer to the averaged total cumulative length and volume of all cylinders per branch as “total length” and “total volume”. To analyse the effect of scanning distance on the lengths and

volumes of the branches, GAMs (*generalised additive models*) were derived using the “mgcv” package (Wood 2011). The total length and volume per branch were modelled as functions of scanning distance using a thin plate spline and branch ID as a random effect. The benchmark data were not included in these models since the pre-processing was not consistent with the experimental data. For each hyperparameter set, a separate set of models for length and volume was modelled. To handle the heteroscedasticity of the data, which showed higher variance with increasing scanning distance, the response variables were log-transformed. The residuals of all four GAMs were successfully checked for normality both visually and using Kolmogorov–Smirnov tests. To account for the bias introduced by log-transformation, correction factors were derived and applied to the back-transformed predictions (Baskerville 1972; Sprugel 1983). Confidence intervals were obtained by bootstrapping each model 1000 times and calculating the 2.5% and the 97.5% quantiles of the respective back-transformed and bias-corrected predictions. To facilitate the interpretation of the results, the cumulative cylinder length and the volume of the branches were divided into 1 cm-diameter classes.

Results

Selected branch characteristics for the benchmark data and for the experimental scans at distances of 20 and 45 m are given in Table 1. The presented values show the arithmetic mean \pm standard deviation for the ten branches. Values used for calculation are the averaged length and volume of the respective 50 QSMs per scanning distance and branch (see Sect. 2.4). Therefore, the standard deviation reflects the variance between the branches caused by different branch architectures and sizes. In general, the dataset based on fixed QSM hyperparameters leads to results closer to the benchmark results. While for the length estimates, the two

parameterisations performed similarly well, the volume estimates differed considerably.

The point cloud resolution of the point clouds varied depending on the different scanning distances (Fig. 3). Displaying a near linear relationship between the scanning distance and the logarithm of the number of points, the number of points per branch decreased logarithmically with increasing scanning distance. At the first scanning distance of 5 m, the point clouds of the branches consisted of 27,681 points on average. At a scanning distance of 45 m, the average number of points decreased to 607. The benchmark data contained an average of 343,448 points per sample branch. As the visual inspection of Fig. 3 shows, the high quality of the benchmark data makes it possible to derive QSMs that model even fine structures such as twigs of a few millimetres in diameter or buds. However, as the scanning distance increased, fine structures could no longer be detected. At greater distances, even coarse structures were no longer fully detected, and the pattern of the laser footprint (see also Fig. 2b) became visible due to the low point cloud density (Fig. 3).

The cumulative length of the branches decreased with increasing scanning distance (Fig. 4). While most of the length in the benchmark data was originally in the smallest diameter class (≤ 1 cm), the thickest diameter class shifted to higher diameters with increasing distance. Although the results are slightly different for the two different parameterisations (fixed and optimised), the overall trend and the changing distribution of the length in the diameter classes along the distances are generally similar.

The largest mean underestimation of cumulative branch length occurred at 45 m scanning distance, where the length was underestimated by 75%, regardless of the parameterisation (Table 2).

Both GAMs on cumulative branch length as a function of distance showed highly significant ($p < 0.001$) effects of scanning distance and branch ID. The model based on the fixed parameter dataset achieved an adjusted R^2 (R^2_{adj}) of

Table 1 Branch characteristics for the benchmark data and for the scans conducted at a distance of 20 m and 45 m

	Benchmark	Distance 20 m		Distance 45 m	
		Fixed	Optimised	Fixed	Optimised
Total cumulative length, in m	30.32 \pm 11.50	19.85 \pm 6.59	19.28 \pm 6.64	7.47 \pm 2.53	7.44 \pm 2.66
Length in smallest diameter class (≤ 1 cm), in %	92.36 \pm 2.48	18.94 \pm 2.82	17.07 \pm 7.38	11.36 \pm 3.26	7.52 \pm 2.80
Length in largest diameter class (> 5 cm), in %	0.00 \pm 0.00	0.23 \pm 0.28	1.19 \pm 2.01	2.26 \pm 2.55	17.10 \pm 14.69
Total volume, in l	1.36 \pm 0.55	3.73 \pm 1.38	5.59 \pm 3.03	3.84 \pm 1.12	8.23 \pm 3.80
Volume in smallest diameter class (≤ 1 cm), in %	71.25 \pm 9.45	3.84 \pm 0.86	3.16 \pm 2.96	0.95 \pm 0.43	0.34 \pm 0.25
Volume in largest diameter class (> 5 cm), in %	0.04 \pm 0.11	3.13 \pm 3.76	8.58 \pm 9.86	8.53 \pm 8.04	38.63 \pm 26.17
Number of cylinders	1951 \pm 1351	283 \pm 96	260 \pm 119	59 \pm 23	46 \pm 19

Values are given for both the dataset with fixed parameters and the dataset with optimised parameters. The values are the arithmetic mean \pm standard deviation over the ten branches

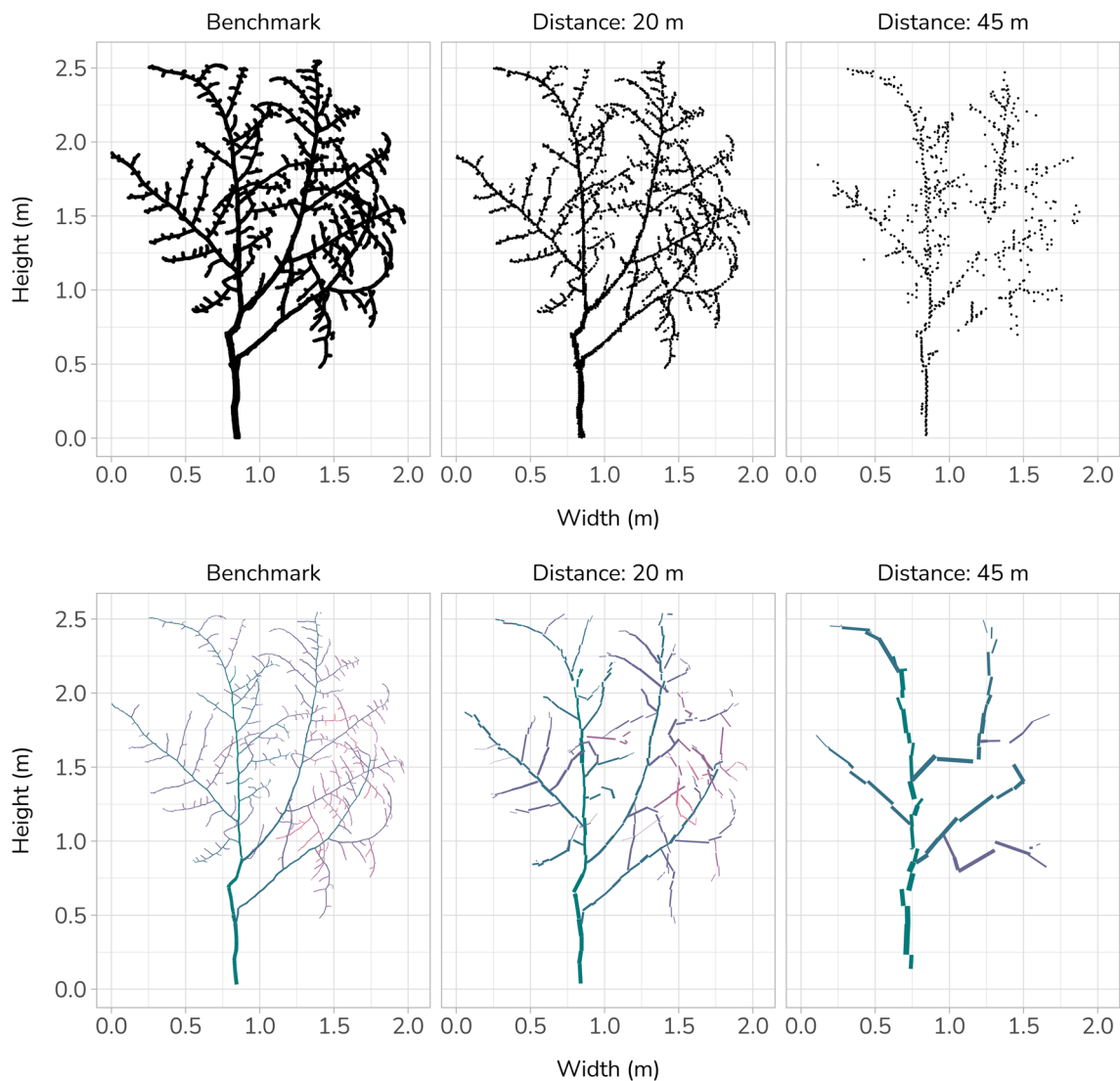


Fig. 3 Point clouds and QSMs of one sample branch scanned from varying distances. The top row shows the point clouds, and the bottom row shows the QSMs of the fixed parameter dataset for the respective distances. The plots on the left show the benchmark data derived from 12 close-range scans, the plots in the centre show the

branch scanned from a distance of 20 m, while the plots on the right show the branch scanned from 45 m distance. The points are transparent to show overlapping points. The QSMs are coloured according to branch order

0.98, explaining 99% of the deviance. The second model achieved a marginally lower R^2_{adj} of 0.97 and explained 98% of the deviance. In both models, the predicted length decreased almost linearly with increasing scanning distance (Fig. 5). For both the raw data and the GAMs, no major differences between the two datasets are apparent.

The total volume of the branches generally increased with scanning distance (Fig. 6). However, the dataset based on the fixed QSM hyperparameters shows a decrease of volume at 45-m scanning distance. While the smallest diameter class (≤ 1 cm) originally accounted for most of the total volume, there is almost no volume within this diameter class at the largest scanning distance. With increasing distances, the

dominant diameter class changes. In contrast to the length estimates, there are large differences between the estimates of the two parametrisations. The dataset using fixed parameters outperformed the dataset using the optimised parameters. The largest average overestimation of branch volume occurred with the optimised parameter dataset and a scanning distance of 45 m, resulting in an overestimation of 539% (see also Table 2) (Fig. 7).

Similar to the previous models, the GAMs regarding branch volume show highly significant ($p < 0.001$) effects of scanning distance and branch ID. The GAM for the fixed parameter dataset reached an R^2_{adj} of 0.83 and explained 85% of the deviance. Here, the model for

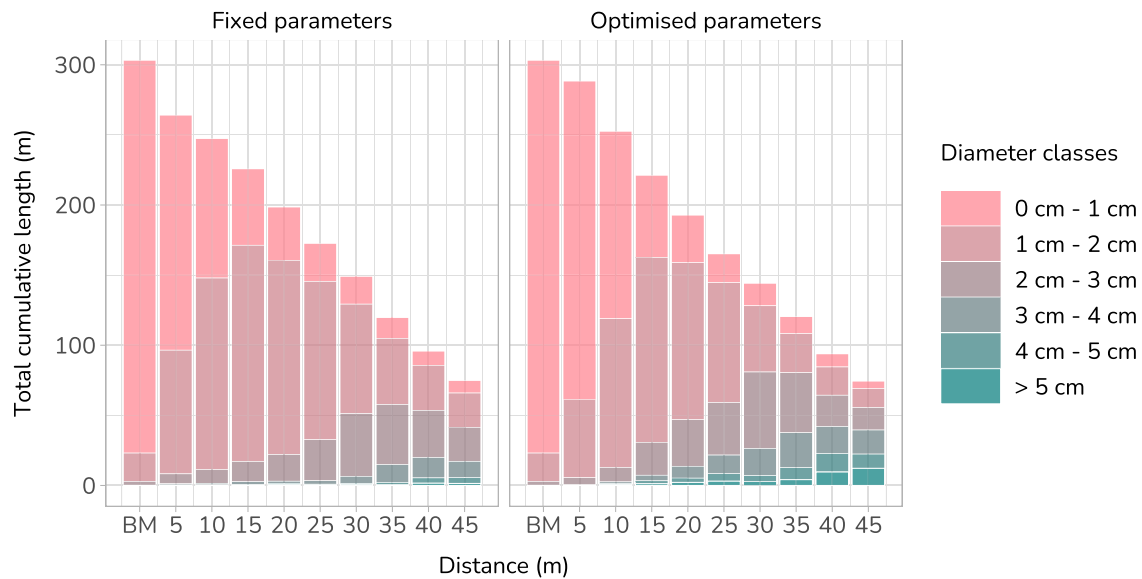


Fig. 4 Total cumulative length of all branches combined (Y-axis) depending on the scanning distance (X-axis) and the cylinder diameter classes (colour). The “BM” bar shows the benchmark data from the 12 close-range scans

Table 2 Average length and volume under/overestimation for the different scanning distances and parameterisations

Distance (m)	Length underestimation (%)		Volume overestimation (%)	
	Fixed	Optimised	Fixed	Optimised
5	-12.67	-4.86	+79.07	+39.39
10	-18.13	-16.63	+123.21	+118.89
15	-24.95	-26.64	+164.37	+237.41
20	-33.77	-35.90	+177.25	+318.41
25	-42.43	-45.24	+191.21	+377.18
30	-50.21	-52.13	+231.29	+404.61
35	-60.21	-59.87	+234.98	+479.45
40	-67.77	-68.63	+268.58	+522.82
45	-74.91	-75.11	+206.56	+539.35

the optimised parameter dataset performed slightly better with an R^2_{adj} of 0.86, explaining 88% of the deviance. While both models show narrow confidence intervals and an almost linear relationship between estimated volume and scanning distance up to a scanning distance of 35 m, they afterwards increasingly diverge (Fig. 5). Above a distance of 35 m, the model based on the fixed parameter dataset shows decreasing volume with increasing distance, while the other model exhibits a monotonic trend of increasing volume. Furthermore, the confidence intervals expand with the scanning distance.

Discussion

In this study, we investigated the effect of scanning distance on the estimated cumulative branch length and total branch volume of ten European beech branches using TLS data and QSMs. Excluding disturbing external factors such as wind and occlusion by the study design, we could extract the influence of distance on point cloud quality. Additionally, the artificial environment with many horizontal and vertical planes facilitated the coregistration of the individual scans, reducing errors resulting from inaccurate coregistration. Given the results of our experiment, we can confirm the initial research hypotheses: As the distance between scanner and branches increases, the cumulative branch length decreases, and the total branch volume increases. While for one of the QSM parameterisations, the volume increased monotonically, the other parameterisation showed an overestimation of the volume at all scan distances, but at 35 m scanning distance, the overestimation culminated and decreased at higher distances. The GAMs for the volume estimates show that uncertainty increases with scanning distance, as shown by the broadening confidence intervals.

This study is an experiment under partially controlled conditions and therefore deviates from reality in some respects. While we depicted the branches in similar distances as in a natural environment, the change from vertical to horizontal distances that should simulate the scanning process in forest surrounding is artificial. Nevertheless, this should not alter the way; the algorithm fits cylinders into the point clouds. Probably, the biggest difference between our study and scanning in forests is the disturbance regime.

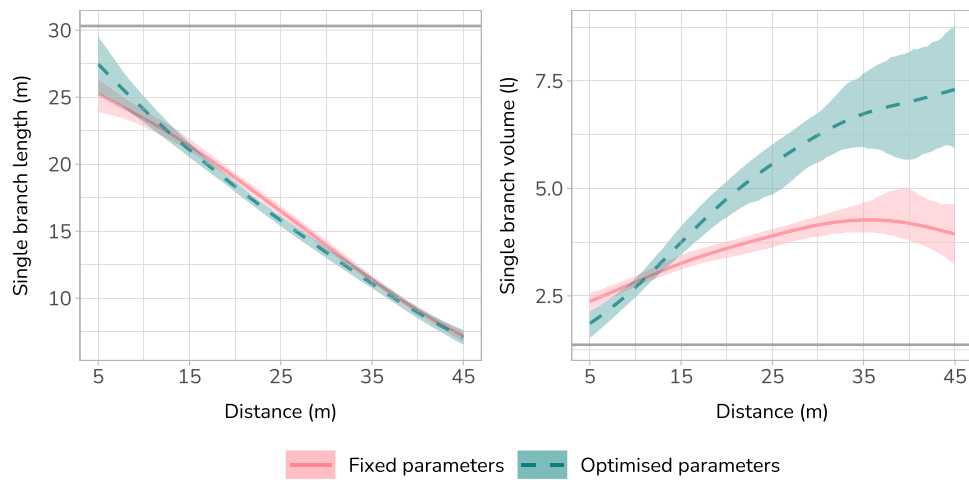


Fig. 5 Regression models predicting the over/underestimation of length (left) and volume (right) of single sample branches as a function of the scanning distance. Separate models were fitted for data derived from QSMs using fixed hyperparameters (pink, solid line) and for data derived from QSMs using optimised hyperparameters

(turquoise, dashed line). The shaded areas indicate the bootstrapped confidence intervals. The effect of the individual branch ID was excluded for the plots. The grey line indicates the mean of the benchmark data

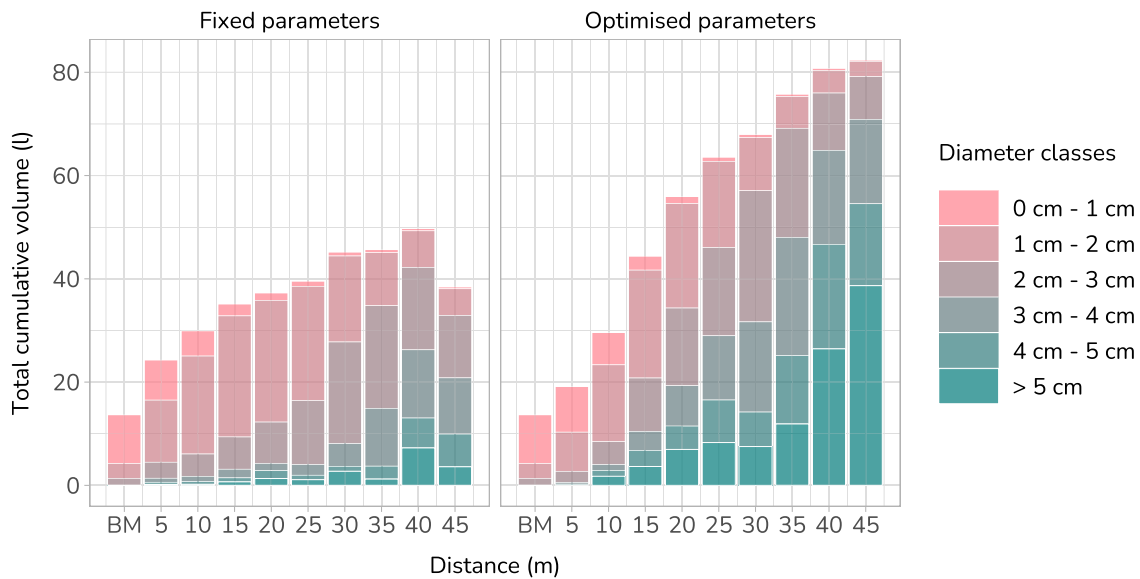


Fig. 6 Total cumulative volume of all branches (Y-axis) depending on the scanning distance (X-axis) and the cylinder diameter classes (colour). The “BM” bar shows the benchmark data from the 12 close-range scans

In natural environments, one must expect wind, humidity and dust particles which all might cause different artefacts (Boehler et al. 2003; Krok et al. 2020). Even slight wind, which is not even detectable from below the canopy, might move branches in the upper crowns (Oliver 1971). Dust particles, insects and pollen can cause returns floating between the branches. Water drops on the TLS device can lead to erroneous data due to reflections and refractions of the outgoing and incoming laser beams (Culvenor et al.

2014; Portillo-Quintero et al. 2014). Moisture on branches might lead to missing returns, as water reduces the amount of reflected light considerably (Kaasalainen et al. 2010), if near-infrared wavelengths are used. Additionally, in our experiment, there was no occlusion by other plant material, which is one of the major problems when trying to depict trees without obstruction (Heinzel and Huber 2017; Schneider et al. 2019; Wang et al. 2019). Depending on stand diameter distribution and density, occlusion can vary and

deteriorate point cloud quality accordingly (Liang et al. 2018), which can be alleviated through a well-chosen scanning setup (Abegg et al. 2017). Occlusion in complex stands is known to affect various derived tree attributes such as height and volume (Liang et al. 2018). All these environmental factors have been excluded in our experimental setup, which was chosen to isolate the distance effect from other environmental influences in the best possible way.

We chose to scan the branches from one side only, as this is the typical perspective of horizontal tree branches scanned with TLS in a real-world setting from an orthogonal perspective. During TLS campaigns, one rarely has the opportunity to scan from a tower or similar structures to capture trees from above. Conversely when using *Airborne Laser Scanning* (ALS) or *UAV Laser Scanning* (ULS), trees are usually only scanned from above, with the ground view lacking (Brede et al. 2017; Wang et al. 2019).

Another source of error is the scanning system used. According to our results, large laser footprints resulting from large distances between scanner and object lead to poor point cloud quality and consequently to poor estimates of the length and volume of fine branch structures. The system used in this study already has a relatively narrow opening angle compared to other TLS devices (Abegg et al. 2023). Furthermore, as the distance between the scanner and the object increases, gaps between individual laser footprints arise, making it more difficult to capture objects from one scanning position entirely (Fig. 2b). Although the RIEGL VZ-400i can operate at higher angular resolutions of up to 0.0007° vertically and 0.0005° horizontally (RIEGL Laser Measurement Systems GmbH 2022), these are generally not used in forestry applications for reasons of time efficiency and practicality. Scanning with higher resolution currently increases the scanning time considerably, which makes data acquisition much more time-consuming and increases the likelihood that the data are negatively affected by environmental factors such as wind. Currently, the availability and quality of LiDAR scanners, regardless of platform, are developing rapidly, and prices are falling. Compared to TLS, mobile laser scanners offer more homogeneous coverage, but also introduce another source of error in the reconstruction of the movement trajectory. ALS and ULS are known to produce lower density point clouds (Calders et al. 2020), which are therefore currently less suitable for QSM reconstruction for fine structures. For this reason, it can be assumed that TLS currently remains the most precise measurement method and that the underestimation of length and overestimation of volume could be even more serious with less precise LiDAR devices as well as with LiDAR measurements from other platforms.

During the pre-processing, we were able to avoid down-sampling, which is commonly applied but may cause additional artefacts. This technique is usually used to reduce the

computational effort, which presents no issue for the small number of branches as in our experiment, but increases rapidly for whole forest stands with mature trees. Down-sampling is sometimes used to homogenise the point cloud density, which is usually heterogeneous in TLS data due to occlusion effects and the distance between laser footprints that vary with scanning distance. Since we did not encounter any occlusion and since each of the point clouds contained only points from similar distances, we assume that our point clouds nevertheless exhibit an approximately uniform point cloud density.

Our results are consistent with those of Abegg et al. (2023), who observed overestimation of small tree volume of more than 100% in a simulation study in a similar scanning environment and using the same QSM reconstruction algorithm. The study by Abegg et al. (2023) concentrates on providing more insights into different scanning systems, without focusing on the cause of the misestimations. Our study sheds light on the observation that sparse data coverage of distant objects leads to missing branch segments and that laser beam diameters exceeding branch diameters lead to a cylinder inflation effect that causes an overestimation of the volume (Demol et al. 2022; Abegg et al. 2023). This cylinder inflation effect is probably caused by partial hits of laser beams. When emitted laser pulses partially hit objects and enough light is reflected to trigger a return, the resulting points may be shifted to the centre of the laser footprint, away from the object (Wilkes et al. 2021). As the scanning distance increases, the size of the footprint increases, potentially increasing the number of partial hits and the introduction of ghost points between objects (Abegg et al. 2021). This is probably the reason why volume estimates deteriorate with increasing scanning distance.

Another factor deteriorating volume estimates is the combination of scatter noise with the lack of data for the branches on the side facing away from the scanner. Since the scanner cannot estimate the angles to the branches in the same accuracy as the distances and since the rear facing surfaces are not depicted, the points might not resemble the curved surface of the branch cylinder, but rather a flat plane. This could lead to an overestimation of cylinder radii caused by minimising the distance between the points and the cylinder surface, as the surface of a large cylinder also locally increasingly resembles a flat plane.

Nevertheless, previous studies found field-based measurements to agree well with TLS-based volume and biomass estimates (Calders et al. 2015; Gonzalez de Tanago et al. 2018). This can probably be explained by the fact that these studies investigated the volume or biomass of mature trees at the tree or stand level. We assume that the overestimation effects were cancelled out by occlusion effects which lead to an underestimation of volume which has already been observed by Kükenbrink et al. (2021).

This is a plausible explanation, as occlusion is typically an important issue especially in the upper crown (Wang et al. 2019), where much of the fine branch structure is located. However, one cannot rely on the assumption that different sources of error will always compensate for each other, as this might not always be the case. Depending on the complexity of a stand, the occlusion and the resulting underestimation vary and might not coincide with the overestimation due to cylinder inflation effects.

As can be seen well in Fig. 3, the errors seen are mainly caused by insufficient data and not by the TreeQSM algorithm itself. The observation that the detection of objects with small diameters is limited and deteriorates with scanning distance is in line with the results of Abegg et al. (2021), who investigated the influence of the laser beam diameter on point cloud quality in a virtual environment. However, as can be seen in Figs. 5 and 6, the errors in the volume estimates vary considerably for different hyperparameters, with the automatically optimised parameters, leading to greater overestimation for distances of about 10 m and more. Apparently, the choice of hyperparameters is a source of uncertainty that needs to be resolved in order to obtain more robust estimates. However, since the errors are mainly attributable to the point cloud quality, there is no point in optimising the algorithm as long as the scanning procedure is not optimised and standardised. Narrower scanning patterns and smaller scanning distances could increase the accuracy of the point cloud at the expense of more labour-intensive fieldwork. However, this approach is limited as it is currently not possible to deploy a TLS close to the canopy or an ULS below the canopy. Therefore, larger scan distances, which are inevitable due to tree height, are unavoidable. The only other option seems to be the use of multi-platform approaches combining top-down and bottom-up scans to provide full coverage through close-range scans.

It should be emphasised that this study focuses on particularly small branches. Volume estimates from TLS data of trunks or larger branches might be much closer to reality (Abegg et al. 2023). Still, identifying and exploring the limitations of the technology might provide a better understanding for which questions could be useful and which applications should be avoided. Currently, we are not aware of any other solution to estimate the volume of trees without destruction, apart from allometric equations, which have their own limitations (Disney et al. 2018), or destructive sampling, which is extremely labour-intensive, as well as species- and site-specific. Therefore, it is crucial to further our understanding of this technology as it is likely to be used in the future owing to its advantages over other methods.

Outlook

It is important to note that European beech as a species is especially challenging to scan due to its very fine branch structure and its large tree heights, which can reach more than 40 m (Packham et al. 2012). However, the branches of beech trees have a relatively straight growth compared to other tree species (e.g. *Quercus* spp.), which is probably an advantage for reconstruction using straight cylinders. We assume that the reconstruction quality might vary considerably between different tree species due to growth differences such as minimum branch diameter, branch curvature, tree height and branch density within the crown. These aspects should be explored in future research to improve our understanding of the mechanisms that influence the accuracy of the estimates between tree species. Taking this into account, it is quite a complex task to provide a calibration to compensate for the severe biases we observe. Such a calibration would have to consider for each cylinder its distance from the scanner, its diameter and length, as well as information about the tree species and the scanning setup, including the scanning device itself as well as its placement and the surrounding environment. In summary, it would be necessary to estimate the errors separately due to the scanner limitations, the tree characteristics and the errors caused by occlusion or prevailing circumstances such as the weather. This is very challenging with a point cloud that is assembled from multiple scans. Even if distance-dependent bias was successfully quantified taking these aspects into account, efforts to derive calibration curves would be complicated by the fact that many cylinders are likely to be fitted to points acquired from different scan distances. Furthermore, correcting the diameter for the individual cylinders while greatly underestimating the branch length would still lead to incorrect estimates of the volume and vice versa.

Conclusions

Our experiment revealed severe misestimations for branch length and volume, which were biased by up to -75% and $+539\%$, respectively, and deteriorated with increasing distance between the scanner and the branches. It should be mentioned that we scanned the branches under near-optimal conditions to minimise the effects of external environmental factors, as the branches were scanned under leaf-off conditions in an enclosed building. Therefore, the branch length and volume estimates are not necessarily applicable under real forest conditions where the environmental conditions will further decrease the quality of the data. As our results show, the combination of TLS and QSMs is not suitable for reconstructing fine branch structures below 3 cm in diameter even at short distances.

This can mainly be attributed to insufficient data quantities due to the scanner characteristics and is most severe for thin branches. This problem could be partially solved by improved software and hardware. Using current technology, higher angular resolution can already be employed to improve data quality, but at the cost of higher operation time and arising disadvantages. Until scanners are available that offer at least an order of magnitude higher accuracy, precision and angular resolution at similar operation times, all studies and applications using this technology should be aware of these limitations and uncertainties. In future research, we need to gain a better understanding of the influences of different tree structures and environmental conditions on the reconstruction to enable a better assessment of the uncertainties associated with the use of QSMs. Better estimates could be obtainable by combining different sensors and platforms (e.g. TLS & ULS), better pre-processing algorithms that take laser properties into account (more confidence in closer and less divergent laser pulses) and partial calibrations. However, all these solutions have their own individual difficulties that must be overcome.

Appendix



Fig. 7 Scanning setup of one set of five branches. The branches were stabilised using platforms and tripods. The scanner was mounted to a trolley to facilitate scanning

Table 3 Overview over the TreeQSM hyperparameters used for the reconstruction of the QSMs of the optimised dataset

Dataset	<i>PatchDiam1</i>		<i>PatchDiam2Min</i>		<i>PatchDiam2Max</i>	
	Min	Max	Min	Max	Min	Max
Benchmark	0.0021	0.0231	0.0008	0.0136	0.0023	0.0302
Distance 5 m	0.0017	0.0226	0.0007	0.0133	0.0018	0.0296
Distance 10 m	0.0019	0.0233	0.0007	0.0138	0.0020	0.0305
Distance 15 m	0.0023	0.0240	0.0009	0.0142	0.0025	0.0314
Distance 20 m	0.0018	0.0241	0.0007	0.0142	0.0019	0.0315
Distance 25 m	0.0016	0.0214	0.0006	0.0126	0.0017	0.0280
Distance 30 m	0.0015	0.0223	0.0006	0.0132	0.0016	0.0292
Distance 35 m	0.0032	0.0185	0.0012	0.0110	0.0034	0.0243
Distance 40 m	0.0015	0.0174	0.0006	0.0103	0.0016	0.0228
Distance 45 m	0.0015	0.0165	0.0006	0.0097	0.0016	0.0216

For each scanning distance, the minimum and maximum values of the parameters *PatchDiam1*, *PatchDiam2Min* and *PatchDiam2Max* across all ten branches are given

Supplementary Information The online version contains supplementary material available at <https://doi.org/10.1007/s10342-023-01651-z>.

Acknowledgements We would like to thank the Department of Sport and Sport Science, University of Freiburg for providing a sports hall for the data collection.

Author contributions We apply for a split first authorship of CM and ZS. Conceptualisation, methodology and writing - original draft preparation were contributed by CM, ZS and JF; CM and ZS did investigation; ZS performed formal analysis and visualisation; Writing - review and editing was done by CM, ZS, JF, JS, KC, MD, FM, PR and TS; CM and TS were involved in funding acquisition.

Funding Open Access funding enabled and organized by Projekt DEAL. Open Access funding enabled and organized by Projekt DEAL. The project INTEGRA is supported by funds of the Federal Ministry of Food and Agriculture (BMEL) based on a decision of the parliament of the Federal Republic of Germany via the Federal Office for Agriculture and Food (BLE) under the Federal Programme for Ecological Farming and Other Forms of Sustainable Agriculture (Support code 2819NA071).

Availability of data and material The datasets generated during and/or analysed during the current study are available from the corresponding author on reasonable request.

Declarations

Conflict of interests The authors have no competing interests to declare that are relevant to the content of this article.

Open Access This article is licensed under a Creative Commons Attribution 4.0 International License, which permits use, sharing, adaptation, distribution and reproduction in any medium or format, as long as you give appropriate credit to the original author(s) and the source, provide a link to the Creative Commons licence, and indicate if changes were made. The images or other third party material in this article are included in the article's Creative Commons licence, unless indicated otherwise in a credit line to the material. If material is not included in the article's Creative Commons licence and your intended use is not permitted by statutory regulation or exceeds the permitted use, you will

need to obtain permission directly from the copyright holder. To view a copy of this licence, visit <http://creativecommons.org/licenses/by/4.0/>.

References

- Abegg M, Boesch R, Schaepman ME, Morsdorf F (2021) Impact of beam diameter and scanning approach on point cloud quality of terrestrial laser scanning in forests. *Geosci Remote Sens IEEE Trans*. <https://doi.org/10.1109/36.92141459:8153-8167.10.1109/TGRS.2020.3037763>
- Abegg M, Bösch R, Kükenbrink D, Morsdorf F (2023) Tree volume estimation with terrestrial laser scanning—testing for bias in a 3D virtual environment. *Agric For Meteorol* 331:109348. <https://doi.org/10.1016/j.agrformet.2023.109348>
- Abegg M, Kükenbrink D, Zell J, Schaepman EM, Morsdorf F (2017) Terrestrial laser scanning for forest inventories—tree diameter distribution and scanner location impact on occlusion. *Forests*, 8. <https://doi.org/10.3390/f8060184>
- Åkerblom M, Raunonen P, Kaasalainen M, Casella E (2015) Analysis of geometric primitives in quantitative structure models of tree stems. *Remote Sens* 7:4581–4603. <https://doi.org/10.3390/rs70404581>
- Antonarakis AS, Richards KS, Brasington J, Muller E (2010) Determining leaf area index and leafy tree roughness using terrestrial laser scanning. *Water Resour Res*, 46. <https://doi.org/10.1029/2009WR008318>
- Astrup R, Ducey MJ, Granhus A, Ritter T, von Lüpke N (2014) Approaches for estimating stand-level volume using terrestrial laser scanning in a single-scan mode. *Can J For Res* 44:666–676. <https://doi.org/10.1139/cjfr-2013-0535>
- Baskerville GL (1972) Use of logarithmic regression in the estimation of plant biomass. *Can J for Res* 2:49–53. <https://doi.org/10.1139/x72-009>
- Boehler W, Bordas Vincent M., Marbs A (2003) Investigating laser scanner accuracy. In: Altan MO (ed) Proceedings of the 19th CIPA Symposium, Antalya, Turkey
- Bohn Reckziegel R, Larysch E, Sheppard JP, Kahle H-P, Morhart C (2021) Modelling and comparing shading effects of 3D tree structures with virtual leaves. *Remote Sens* 13:532. <https://doi.org/10.3390/rs13030532>
- Bohn Reckziegel R, Sheppard JP, Kahle H-P, Larysch E, Spiecker H, Seifert T, Morhart C (2022) Virtual pruning of 3D trees as a tool

- for managing shading effects in agroforestry systems. *Agrofor Syst* 96:89–104. <https://doi.org/10.1007/s10457-021-00697-5>
- Brede B, Lau A, Bartholomeus HM, Kooistra L (2017) Comparing RIEGL RiCOPTER UAV LiDAR derived canopy height and DBH with terrestrial LiDAR. *Sensors (Basel)* 17. <https://doi.org/10.3390/s17102371>
- Calders K, Newnham G, Burt A, Murphy S, Raunonen P, Herold M, Culvenor D, Avitabile V, Disney M, Armston J (2015) Non-destructive estimates of above-ground biomass using terrestrial laser scanning. *Methods Ecol Evol* 6:198–208. <https://doi.org/10.1111/2041-210X.12301>
- Calders K, Adams J, Armston J, Bartholomeus H, Bauwens S, Bentley LP, Chave J, Danson FM, Demol M, Disney M, Gaulton R, Krishna Moorthy SM, Levick SR, Saarinen N, Schaaf C, Stovall A, Terry L, Wilkes P, Verbeeck H (2020) Terrestrial laser scanning in forest ecology: expanding the horizon. *Remote Sens Environ* 251:112102. <https://doi.org/10.1016/j.rse.2020.112102>
- Calders K, Verbeeck H, Burt A, Origo N, Nightingale J, Malhi Y, Wilkes P, Raunonen P, Bunce RG, Disney M (2022) Laser scanning reveals potential underestimation of biomass carbon in temperate forest. *Ecol Sol Evidence*, 3. <https://doi.org/10.1002/2688-8319.12197>
- CloudCompare (2022) CloudCompare. <http://www.cloudcompare.org/>
- Culvenor DS, Newnham GJ, Mellor A, Sims NC, Haywood A (2014) Automated in-situ laser scanner for monitoring forest Leaf Area Index. *Sensors (Basel)* 14:14994–15008. <https://doi.org/10.3390/s140814994>
- Demol M, Wilkes P, Raunonen P, Krishna Moorthy SM, Calderys K, Gielen B, Verbeeck H (2022) Volumetric overestimation of small branches in 3D reconstructions of *Fraxinus excelsior*. *Silva Fennica* 56. <https://doi.org/10.14214/sf.10550>
- Disney MI, Boni Vicari M, Burt A, Calderys K, Lewis SL, Raunonen P, Wilkes P (2018) Weighing trees with lasers: advances, challenges and opportunities. *Interface Focus*, 8. <https://doi.org/10.1098/rsfs.2017.0048>
- Ehbrecht M, Schall P, Juchheim J, Ammer C, Seidel D (2016) Effective number of layers: a new measure for quantifying three-dimensional stand structure based on sampling with terrestrial LiDAR. *Adaptation of forests and forest management to changing climate selected papers from the conference on “Adaptation of Forests and Forest Management to Changing Climate with Emphasis on Forest Health: A Review of Science, Policies and Practices”*, Umeå, Sweden, August 25–28, 2008 380:212–223. <https://doi.org/10.1016/j.foreco.2016.09.003>
- Ehbrecht M, Schall P, Ammer C, Fischer M, Seidel D (2019) Effects of structural heterogeneity on the diurnal temperature range in temperate forest ecosystems. *Adaptation of Forests and Forest Management to Changing Climate Selected papers from the conference on “Adaptation of Forests and Forest Management to Changing Climate with Emphasis on Forest Health: A Review of Science, Policies and Practices”*, Umeå, Sweden, August 25–28, 2008 432:860–867. <https://doi.org/10.1016/j.foreco.2018.10.008>
- Frey J, Asbeck T, Bausch J (2020) Predicting tree-related microhabitats by multisensor close-range remote sensing structural parameters for the selection of retention elements. *Remote Sens* 12:867. <https://doi.org/10.3390/rs12050867>
- Gonzalez de Tanago J, Lau A, Bartholomeus H, Herold M, Avitabile V, Raunonen P, Martius C, Goodman RC, Disney M, Manuri S, Burt A, Calderys K (2018) Estimation of above-ground biomass of large tropical trees with terrestrial LiDAR. *Methods Ecol Evol* 9:223–234. <https://doi.org/10.1111/2041-210X.12904>
- Haala N, Reulke R, Thies M, Aschoff T (2004) Combination of terrestrial Laser Scanning with high resolution panoramic Images for Investigations in Forest Applications and tree species recognition. In: Maas H-G, Schneider D (eds) *Panoramic Photogrammetry Workshop, IAPRS - XXXIV*
- Hackenberg J, Morhart C, Sheppard JP, Spiecker H, Disney M (2014) Highly accurate tree models derived from terrestrial laser scan data: a method description. *Forests* 5:1069–1105. <https://doi.org/10.3390/f5051069>
- Hackenberg J, Spiecker H, Calderys K, Disney M, Raunonen P (2015) SimpleTree—an efficient open source tool to build tree models from TLS clouds. *Forests* 6:4245–4294. <https://doi.org/10.3390/f6114245>
- Heinzel J, Huber M (2017) Detecting tree stems from volumetric TLS data in forest environments with rich understory. *Remote Sens* 9:9. <https://doi.org/10.3390/rs9010009>
- Helbach J, Frey J, Messier C, Mörsdorf M, Scherer-Lorenzen M (2022) Light heterogeneity affects understory plant species richness in temperate forests supporting the heterogeneity-diversity hypothesis. *Ecol Evol* 12:e8534. <https://doi.org/10.1002/ece3.8534>
- Kaasalainen S, Niittymäki H, Krooks A, Koch K, Kaartinen H, Vain A, Hyyppä H (2010) Effect of target moisture on laser scanner intensity. *Geosci Remote Sens IEEE Trans*. <https://doi.org/10.1109/36.92141448:2128-2136.10.1109/TGRS.2009.2036841>
- Knuff AK, Staab M, Frey J, Dormann CF, Asbeck T, Klein A-M (2020) Insect abundance in managed forests benefits from multi-layered vegetation. *Basic Appl Ecol* 48:124–135. <https://doi.org/10.1016/j.baae.2020.09.002>
- Kolbe S, Rentschler F, Frey J, Seifert T, Gardiner B, Detter A, Schindler D (2022) Assessment of effective wind loads on individual plantation-grown forest trees. *Forests* 13:1026. <https://doi.org/10.3390/f13071026>
- Kretschmer U, Kirchner N, Morhart C, Spiecker H (2013) A new approach to assessing tree stem quality characteristics using terrestrial laser scans. *Silva Fennica* 47:1–14. <https://doi.org/10.14214/sf.1071>
- Krok G, Kraszewski B, Stereńczak K (2020) Application of terrestrial laser scanning in forest inventory—an overview of selected issues. *For Res Pap* 81:175–194. <https://doi.org/10.2478/frp-2020-0021>
- Kükenbrink D, Gardi O, Mörsdorf F, Thüing E, Schellenberger A, Mathys L (2021) Above-ground biomass references for urban trees from terrestrial laser scanning data. *Ann Bot* 128:709–724. <https://doi.org/10.1093/aob/mcab002>
- Lau A, Martius C, Bartholomeus H, Shenkin A, Jackson T, Malhi Y, Herold M, Bentley LP (2019) Estimating architecture-based metabolic scaling exponents of tropical trees using terrestrial LiDAR and 3D modelling. *For Ecol Manage* 439:132–145. <https://doi.org/10.1016/j.foreco.2019.02.019>
- Liang X, Kankare V, Hyyppä J, Wang Y, Kukko A, Haggrén H, Yu X, Kaartinen H, Jaakkola A, Guan F, Holopainen M, Vastaranta M (2016) Terrestrial laser scanning in forest inventories. Theme Issue “state-of-the-Art in Photogrammetry, Remote Sensing and Spatial Information Science” 115:63–77. <https://doi.org/10.1016/j.isprsjprs.2016.01.006>
- Liang X, Hyyppä J, Kaartinen H, Lehtomäki M, Pyörälä J, Pfeifer N, Holopainen M, Broly G, Francesco P, Hackenberg J, Huang H, Jo H-W, Katoh M, Liu L, Mokroš M, Morel J, Olofsson K, Poveda-Lopez J, Trochta J, Wang Di, Wang J, Xi Z, Yang B, Zheng G, Kankare V, Luoma V, Yu X, Chen L, Vastaranta M, Saarinen N, Wang Y (2018) International benchmarking of terrestrial laser scanning approaches for forest inventories. Theme Issue “state-of-the-Art in Photogrammetry, Remote Sensing and Spatial Information Science” 144:137–179. <https://doi.org/10.1016/j.isprsjprs.2018.06.021>
- Maack J, Lingenfelder M, Weinacker H, Koch B (2016) Modelling the standing timber volume of Baden-Württemberg—a large-scale approach using a fusion of Landsat, airborne LiDAR and National

- Forest Inventory data. *Int J Appl Earth Obs Geoinf* 49:107–116. <https://doi.org/10.1016/j.jag.2016.02.004>
- Oliver HR (1971) Wind profiles in and above a forest canopy. *Q J R Meteorol Soc* 97:548–553. <https://doi.org/10.1002/qj.49709741414>
- Othmani A, Lew Yan Voon LFC, Stolz C, Piboule A (2013) Single tree species classification from Terrestrial Laser Scanning data for forest inventory. *Pattern Recogn Lett* 34:2144–2150. <https://doi.org/10.1016/j.patrec.2013.08.004>
- Packham JR, Thomas PA, Atkinson MD, Degen T (2012) Biological flora of the British Isles: *Fagus sylvatica*. *J Ecol* 100:1557–1608. <https://doi.org/10.1111/j.1365-2745.2012.02017.x>
- Paul KI, Roxburgh SH, Chave J, England JR, Zerihun A, Specht A, Lewis T, Bennett LT, Baker TG, Adams MA, Huxtable D, Montagu KD, Falster DS, Feller M, Sochacki S, Ritson P, Bastin G, Bartle J, Wildy D, Hobbs T, Larmour J, Waterworth R, Stewart HTL, Jonson J, Forrester DI, Applegate G, Mendham D, Bradford M, O’Grady A, Green D, Sudmeyer R, Rance SJ, Turner J, Barton C, Wenk EH, Grove T, Attiwill PM, Pinkard E, Butler D, Brooksbank K, Spencer B, Snowdon P, O’Brien N, Battaglia M, Cameron DM, Hamilton S, McAuthur G, Sinclair J (2016) Testing the generality of above-ground biomass allometry across plant functional types at the continent scale. *Glob Change Biol* 22:2106–2124. <https://doi.org/10.1111/gcb.13201>
- Picard N, Boyemba Bosela F, Rossi V (2015) Reducing the error in biomass estimates strongly depends on model selection. *Ann For Sci* 72:811–823. <https://doi.org/10.1007/s13595-014-0434-9>
- Picard N, Saint-André L, Henry M (2012) Manual for building tree volume and biomass allometric equations: from field measurement to prediction. Food and Agricultural Organization of the United Nations and Centre de Coopération Internationale en Recherche Agronomique pour le Développement, Rome, Montpellier
- Portillo-Quintero C, Sanchez-Azofeifa A, Culvenor D (2014) Using VEGNET In-Situ Monitoring LiDAR (IML) to capture dynamics of plant area index, structure and phenology in Aspen Parkland Forests in Alberta, Canada. *Forests* 5:1053–1068. <https://doi.org/10.3390/f5051053>
- Pretzsch H, Seifert S, Huang P (2011) Beitrag des terrestrischen Laser-scannings zur Erfassung der Struktur von Baumkronen | Application of terrestrial laser scanning for measuring tree crown structures. *Swiss For J* 162:186–194. <https://doi.org/10.3188/szf.2011.0186>
- Puliti S, Breidenbach J, Astrup R (2020) Estimation of forest growing stock volume with UAV laser scanning data: can it be done without field data? *Remote Sens* 12:1245. <https://doi.org/10.3390/rs12081245>
- Pyörälä J, Kankare V, Liang X, Saarinen N, Rikala J, Kivinen V-P, Sipi M, Holopainen M, Hyypää J, Vastaranta M (2019) Assessing log geometry and wood quality in standing timber using terrestrial laser-scanning point clouds. *Forestry* 92:177–187. <https://doi.org/10.1093/forestry/cpy044>
- R Core Team (2022) R: A language and environment for statistical computing. <https://www.R-project.org/>
- Rappa NJ, Staab M, Frey J, Winiger N, Klein A-M (2022) Multiple forest structural elements are needed to promote beetle biomass, diversity and abundance. *Forest Ecosyst* 9:100056. <https://doi.org/10.1016/j.fecs.2022.100056>
- Raumonen P, Kaasalainen M, Åkerblom M, Kaasalainen S, Kaartinen H, Vastaranta M, Holopainen M, Disney M, Lewis P (2013) Fast automatic precision tree models from terrestrial laser scanner data. *Remote Sens* 5:491–520. <https://doi.org/10.3390/rs5020491>
- Raumonen P, Åkerblom M (2022) InverseTampere/TreeQSM: Version 2.4.1. Zenodo
- Raumonen P, Casella E, Calders K, Murphy S, Åkerblom M, Kaasalainen M (2015) Massive-scale tree modelling from TLS data. *ISPRS Ann. Photogramm. Remote Sens Spatial Inf Sci* II-3/W4:189–196. <https://doi.org/10.5194/isprs-annals-II-3-W4-189-2015>
- RIEGL Laser Measurement Systems GmbH (2022): Data Sheet, RIEGL VZ-400i. http://www.riegl.com/uploads/tx_pxpriegldo_wnloads/RIEGL_VZ-400i_Datasheet_2022-09-27.pdf
- Roskopf E, Morhart C, Nahm M (2017) Modelling Shadow Using 3D Tree Models in High Spatial and Temporal Resolution. *Remote Sens*, 9. <https://doi.org/10.3390/rs9070719>
- Roxburgh SH, Paul KI, Clifford D, England JR, Raison RJ (2015) Guidelines for constructing allometric models for the prediction of woody biomass: How many individuals to harvest? *Ecosphere* 6:art38. <https://doi.org/10.1890/ES14-00251.1>
- Schindler Z, Seifert T, Sheppard JP, Morhart C (2023a) Allometric models for above-ground biomass, carbon and nutrient content of wild cherry (*Prunus avium* L.) trees in agroforestry systems. *Ann For Sci*, 80. <https://doi.org/10.1186/s13595-023-01196-6>
- Schindler Z, Morhart C, Sheppard JP, Frey J, Seifert T (2023b) In a nutshell: Exploring single tree parameters and above-ground carbon sequestration potential of common walnut (*Juglans regia* L.) in agroforestry systems. *Agroforestry Syst.* <https://doi.org/10.1007/s10457-023-00844-0>
- Schneider FD, Kükenbrink D, Schaepman ME, Schimel DS, Morsdorf F (2019) Quantifying 3D structure and occlusion in dense tropical and temperate forests using close-range LiDAR. *Agric For Meteorol* 268:249–257. <https://doi.org/10.1016/j.agrformet.2019.01.033>
- Seifert T, Seifert S (2014) Modelling and simulation of tree biomass. In: Seifert T (ed) *Bioenergy from wood: sustainable production in the tropics*. Springer, Netherlands, pp 43–65
- Sheppard JP, Morhart C, Hackenberg J, Spiecker H (2017) Terrestrial laser scanning as a tool for assessing tree growth. *iForest* 10:172–179. <https://doi.org/10.3832/ifor2138-009>
- Sileshi GW (2014) A critical review of forest biomass estimation models, common mistakes and corrective measures. *Adaptation of Forests and Forest Management to Changing Climate Selected papers from the conference on “Adaptation of Forests and Forest Management to Changing Climate with Emphasis on Forest Health: A Review of Science, Policies and Practices”*, Umeå, Sweden, August 25–28, 2008 329:237–254. <https://doi.org/10.1016/j.foreco.2014.06.026>
- Sprugel DG (1983) Correcting for bias in log-transformed allometric equations. *Ecology* 64:209–210. <https://doi.org/10.2307/1937343>
- Stovall AEL, Masters B, Fatoyinbo L, Yang X (2021) TLSLeAF: automatic leaf angle estimates from single-scan terrestrial laser scanning. *New Phytol* 232:1876–1892. <https://doi.org/10.1111/nph.17548>
- van der Zande D, Stuckens J, Verstraeten WW, Muys B, Coppin P (2010) Assessment of light environment variability in broad-leaved forest canopies using terrestrial laser scanning. *Remote Sens* 2:1564–1574. <https://doi.org/10.3390/rs2061564>
- Vonderach C, Voegtle T, Adler P (2012) Voxel-based approach for estimating urban tree volume from terrestrial laser scanning data. *Int Arch Photogramm Remote Sens Spatial Inf. Sci.* XXXIX-B8:451–456. <https://doi.org/10.5194/isprsarchives-XXXIX-B8-451-2012>
- Wang Y, Lehtomäki M, Liang X, Pyörälä J, Kukko A, Jaakkola A, Liu J, Feng Z, Chen R, Hyypää J (2019) Is field-measured tree height as reliable as believed—a comparison study of tree height estimates from field measurement, airborne laser scanning and terrestrial laser scanning in a boreal forest. Theme Issue “state-of-the-Art in Photogrammetry, Remote Sensing and Spatial

- Information Science” 147:132–145. <https://doi.org/10.1016/j.isprsjprs.2018.11.008>
- Wilkes P, Shenkin A, Disney M, Malhi Y, Bentley LP, Vicari MB (2021) Terrestrial laser scanning to reconstruct branch architecture from harvested branches. *Methods Ecol Evol* 12:2487–2500. <https://doi.org/10.1111/2041-210X.13709>
- Wood SN (2011) Fast stable restricted maximum likelihood and marginal likelihood estimation of semiparametric generalized linear models. *J Roy Stat Soc Ser B (Statistical Methodology)* 73:3–36. <https://doi.org/10.1111/j.1467-9868.2010.00749.x>
- Yrttimaa T, Junttila S, Luoma V, Calders K, Kankare V, Saarinen N, Kukko A, Holopainen M, Hyyppä J, Vastaranta M (2023) Capturing seasonal radial growth of boreal trees with terrestrial laser scanning. *Adaptation of Forests and Forest Management to Changing Climate Selected papers from the conference on “Adaptation of Forests and Forest Management to Changing Climate with Emphasis on Forest Health: A Review of Science, Policies and Practices”*, Umeå, Sweden, August 25–28, 2008 529:120733. <https://doi.org/10.1016/j.foreco.2022.120733>

Publisher's Note Springer Nature remains neutral with regard to jurisdictional claims in published maps and institutional affiliations.